A 440-Year Reconstruction of Heavy Precipitation in California from Blue Oak Tree Rings

IAN M. HOWARD,[a] DAVID W. STAHLE,[a] MICHAEL D. DETTINGER,[b] CODY POULSEN,[b] F. MARTIN RALPH,[b] MAX C. A. TORBENSON,[c] AND ALEXANDER GERSHUNOV[b]

[a] *Department of Geosciences, University of Arkansas, Fayetteville, Arkansas*
[b] *Center for Western Weather and Water Extremes, Scripps Institution of Oceanography, La Jolla, California*
[c] *Department of Geography, Johannes Gutenberg University, Mainz, Germany*

(Manuscript received 25 April 2022, in final form 28 November 2022)

ABSTRACT: The variability of water year precipitation and selected blue oak tree-ring chronologies in California are both dominated by heavy precipitation delivered during just a few days each year. These heavy precipitation events can spell the difference between surplus or deficit water supply and elevated flood risk. Some blue oak chronologies are highly correlated with water year precipitation ($r = 0.84$) but are equally well correlated ($r = 0.82$) with heavy precipitation totals ≥25.4 mm (1 in., ≈95th percentile of daily totals, 1949–2004). The blue oak correlation with nonheavy daily totals is much weaker (<25.4 mm; $r = 0.55$). Consequently, some blue oak chronologies represent selective proxies for the temporal and spatial variability of heavy precipitation totals and are used to reconstruct the amount and number of days with heavy precipitation in northern California from 1582 to 2021. Instrumental and reconstructed heavy precipitation totals are strongly correlated with gridded atmospheric river–related precipitation over the western United States, especially in central California. Spectral analysis indicates that instrumental heavy precipitation totals may be dominated by high-frequency variability and the nonheavy totals by low-frequency variance. The reconstruction of heavy precipitation is coherent with instrumental heavy totals across the frequency domain and include concentrations of variance at ENSO and biennial frequencies. Return period analyses calculated using instrumental heavy precipitation totals are representative of the return periods in the blue oak reconstruction despite the large differences in series length. Decadal surges in the amount, frequency, and interannual volatility of heavy precipitation totals are reconstructed, likely reflecting episodes of elevated atmospheric river activity in the past.

SIGNIFICANCE STATEMENT: Tree-ring chronologies of blue oak are highly correlated with precipitation delivered to northern California during just the heaviest days of precipitation each year. The reconstruction of heavy precipitation indicates decadal episodes with a high frequency of extreme precipitation. These episodes of frequent heavy precipitation likely arose because of elevated atmospheric river activity and are relevant to the analysis of water supply and flood hazard in California.

KEYWORDS: Climate variability; Paleoclimate; Atmospheric river; Extreme events; tree rings

1. Introduction

The interannual and decadal variability of water year precipitation in California is dominated by a few daily totals each year in the upper 5th percentile of days with measurable precipitation, including over the catchment of the Sacramento–San Joaquin Delta (Dettinger and Cayan 2014). These heavy storm totals are frequently delivered via landfalling atmospheric rivers (ARs) and are important to water supply and flood risk in the western United States. Droughts in California often arise due to the lack of just a few heavy precipitation days during the winter wet season, while they often end with the precipitation delivered in just one or two large, long-duration, moisture-laden storms (Dettinger 2013; Dettinger and Cayan 2014). These heavy AR storm events have also generated many of the most extreme and costly floods in California history (Corringham et al. 2019). Climate models project that the number and intensity of ARs making landfall on the West Coast of the United States will increase in the coming century due to anthropogenic warming (Dettinger et al. 2011; Warner et al. 2015; Gao et al. 2015; Gershunov et al. 2019), leading to greater flood risks and damages in California (Dettinger et al. 2016; Corringham et al. 2019). A subset of tree-ring chronologies that are strongly correlated with just the heaviest rainfall totals each water year have been discovered in California. These unique proxies can provide a centuries-long paleoclimate perspective on heavy precipitation totals, atmospheric rivers, and the projected future increases in precipitation extremes due to anthropogenic climate and land surface changes.

Blue oak (*Quercus douglasii*) is a California endemic tree species found at the lower forest border on foothills of the Coast Ranges and Sierra Nevada (Pavlik et al. 1991). Exactly dated ring-width chronologies up to 700 years long have been developed using core samples extracted nondestructively from living trees and cross sections cut from dead blue oak wood (Stahle et al. 2013). Some blue oak chronologies are extremely well correlated with water year precipitation (e.g., $r \geq 0.90$) and have been used to reconstruct precipitation (Meko et al. 2011;

Denotes content that is immediately available upon publication as open access.

Corresponding author: Ian M. Howard, ihowardksu@gmail.com

DOI: 10.1175/JHM-D-22-0062.1

Griffin and Anchukaitis 2014), streamflow (Meko et al. 2001), and salinity variations in San Francisco Bay (Stahle et al. 2001).

Moisture sensitive ring-width chronologies have been referred to informally as "integrating pluviometers" because they are often well correlated with precipitation summed for the growing season or even over the entire water year. In California, however, where annual precipitation variability is dominated by the extremes delivered during just a few heavy storms, some moisture-sensitive blue oak chronologies from lower elevation sites where annual precipitation is primarily rain rather than snow are also very highly correlated with precipitation delivered in just a few daily storm extremes. In fact, these blue oak chronologies are well correlated with precipitation summed only for the wettest days and are only modestly correlated with precipitation summed for all remaining days of the year. These selected blue oak chronologies may essentially represent selective proxies for heavy-storm-delivered precipitation in California.

In this study, three selected blue oak chronologies in the Coast Ranges near San Francisco have been used to reconstruct heavy and extreme precipitation amounts in the watershed of the Sacramento River for the past 440 years (1582–2021). The regional average of these tree-ring chronologies is very highly correlated with the sum of precipitation measured on only the days receiving at least 25.4 mm (1 in.) during the water year (r = 0.82; 1949–2004). The derived tree-ring reconstruction of heavy daily precipitation totals (≥25.4 mm, the approximate 95th percentile) can be validated against independent instrumental measurements of heavy precipitation. Because the sum of precipitation measured on these wettest days is very highly correlated with the number of days in each water year with ≥25.4 mm, the blue oak data are also used to estimate the number of days per year with heavy precipitation at or above the 25.4 mm threshold. The derived blue oak reconstructions provide a multicentury perspective on this dynamic fraction of water year precipitation in California, approximately 75% of which is delivered during landfalling atmospheric rivers in the Sacramento River watershed (calculated below).

Steinschneider et al. (2016, 2018) and Borkotoky et al. (2021) have used tree-ring-reconstructed Palmer drought severity index (PDSI) and standardized precipitation index (SPI) to estimate the frequency of extreme precipitation occurrence over California and western North America. These occurrence estimates consider all available tree-ring chronologies in the gridded reconstructions of PDSI and SPI, and the blue oak chronologies from California likely contribute to the skill demonstrated in their reconstructions. However, the discrimination of response to heavy and nonheavy precipitation documented below for blue oak may provide a useful alternative approach that can permit the direct reconstruction of heavy precipitation totals in California. The heavy precipitation reconstruction developed for this research is used to explore the recurrence intervals between extremes, the interannual volatility of extremes, and the multidecadal episodes of elevated heavy precipitation over the past 440 years.

2. Data and methods

a. Instrumental daily precipitation data

The Climate Prediction Center (CPC) gridded unified daily precipitation dataset available from 1948 to present (Higgins et al. 2000, 2007) is used for this analysis and reconstruction of heavy daily precipitation totals in northern California. The CPC grid point data (0.25° resolution) were averaged for a study area in the Sacramento River basin (38.25°–40°N, 120.125°–121.75°W). This study region was chosen because it approximates the area of highest correlation between an average of the three blue oak chronologies and heavy (>95th percentile) precipitation. The 95th percentile for all days with greater than zero precipitation for this study region is 24.20 mm, but for the purposes of this analysis a heavy precipitation day is considered greater than 1 in. (or 25.4 mm, which is the 95.4th percentile of all precipitation days). Instrumental time series of heavy (≥25.4 mm), nonheavy (<25.4 mm), and water year precipitation totals (>0.00 mm) were then computed for the study region. Instrumental heavy precipitation and a regional blue oak chronology were correlated with gridded heavy, nonheavy, and water year precipitation totals over the western United States. Precipitation was first summed at each grid point on the days identified each year in the study area when precipitation was ≥25.4 mm (heavy), <25.4 mm (nonheavy), and >0.00 mm (water year total) and those totals were correlated with study area instrumental heavy precipitation series and the blue oak chronology.

The number of days each year when ≥25.4 mm of precipitation was recorded for the study area was also computed. Gridded precipitation amounts and counts of days from Livneh et al. (2013) were appended to the CPC data before 1948 to illustrate daily precipitation variations from 1916 to 1947. The CPC and Livneh et al. (2013) daily precipitation datasets for the study area are very highly correlated over the common interval from 1949 to 2011 (r = 0.96). The comparisons with the tree-ring data were confined to the period from 1949 to 2004 because the tree-ring chronologies end in 2004 and the high-quality CPC gridded daily observations are available beginning with the water year of 1948–49.

A time series of landfalling atmospheric rivers on the California coast at the Golden Gate (approximately 37.5°N, 122.33°W) at subdaily resolution was used to compare with each heavy precipitation day ≥25.4 mm in the study area. An AR was identified at each location when the integrated vapor transport amount exceeded 250 kg m^{-1} s^{-1} (Rutz and Steenburgh 2014). The presence or absence of AR conditions was computed four times per day from the hourly data (i.e., 0000, 0600, 1200, and 1800 UTC), but if AR conditions were identified for any one of the four daily time steps, that day was considered to have been an AR day for the purposes of this comparison. ARs were detected during 74% of the days with ≥25.4 mm of precipitation in the study area, but only on 45% of days with ≤25.4 mm. If an AR day was identified only when all four hourly time steps were classified as AR conditions, they were detected on 34% of the days with ≥25.4 mm.

For a spatial perspective on the AR signal in the instrumental and proxy data, the heavy precipitation and blue oak time series were correlated with the gridded atmospheric river–related

precipitation totals computed by Gershunov et al. (2017). Gridded counts of AR days each year can also be derived from the Gershunov et al. (2017) dataset as the number of daily totals >0.00 mm. AR-related precipitation totals and the number of AR days each year were both correlated with instrumental heavy precipitation and the blue oak chronology from 1949 to 2004 by first identifying the specific days each year when ≥25.4 mm of precipitation were measured for the study area. Those days were then used to sum AR-related precipitation (and AR days) at each grid point in the Gershunov et al. (2017) dataset prior to correlation with heavy precipitation in the study area and the regional blue oak chronology. The correlations are very similar for AR-related totals and AR days. The spatial correlation with the gridded AR count on days of nonheavy precipitation is also mapped. A comparison of AR count at the coast from the Rutz et al. (2014) dataset with a photomicrograph of blue oak annual rings is presented to illustrate the proportionality between oak growth and ARs.

b. *Tree-ring data*

The blue oak ring width chronologies from Pacheco Pass State Park, Mount Diablo State Park, and Putah Creek (locations specified below) were used for the reconstruction of heavy precipitation. Exploratory analysis of all available blue oak chronologies from northern California indicates that these three series are highly correlated with heavy precipitation but are only modestly correlated with nonheavy totals over the study area. The dated ring width measurements based on 293 radii from 140 trees were detrended and standardized using the computer program ARSTAN (Cook and Krusic 2005, Cook et al. 2017). The autoregressively modeled white noise residual chronology was used for each site because no significant low-order autocorrelation was detected in the time series of instrumental heavy precipitation amounts. The three residual chronologies were averaged to produce the regional blue oak chronology.

The regional blue oak chronology was regressed with the time series of heavy precipitation totals ≥25.4 mm to develop a transfer function to estimate past values of heavy precipitation from the ring-width chronology (Fritts 1976). The instrumental heavy precipitation data were first square root transformed to reduce skewness. Since the tree-ring chronology values are relatively close to zero, regression on nontransformed heavy precipitation data can result in negative reconstructed values. Transformation of the predictand data prevents negative estimates of heavy precipitation. Three calibration experiments were performed using the full time period in common to the ring width and precipitation data (1949–2004), and two subperiods (1949–76, 1977–2004). The two subperiod calibrations were compared with independent instrumental observations of heavy precipitation to provide a measure of statistical validation of the reconstruction models. The full common interval was used to compute the reconstruction of heavy precipitation. Those estimates were then back-transformed (i.e., squared) and the variance lost in regression was restored (by the ratio of observed and reconstructed variances) to complete the final reconstruction in the original units of precipitation.

The instrumental time series of heavy precipitation totals is very highly correlated with the number of days each year with precipitation at or above the threshold of 25.4 mm ($r = 0.96$). Therefore, it was also possible to use the reconstruction of heavy precipitation totals to develop a reconstruction of the number of days each year with precipitation ≥ 25.4 mm. Calibration and validation experiments were performed for the number of heavy daily totals as they were calculated for the heavy daily sums (i.e., 1949–2004, 1949–76, and 1977–2004). The results for the reconstruction of heavy precipitation and the number of days each year with totals above the threshold are both reported below. The reconstruction of the frequency (i.e., number of days) of heavy precipitation each year is not just a semantic difference from the reconstruction of heavy precipitation totals. It provides another way to explain the relationship between heavy precipitation and blue oak growth because the link between the frequency and amount of precipitation delivered during the extremes is very strong in the instrumental data and the days when heavy precipitation happens in the study area are often days when landfalling atmospheric rivers were also observed.

Periodograms of instrumental and reconstructed precipitation were calculated using a discrete Fourier transform of each time series (Bloomfield 2000). The periodograms were smoothed using Daniell filters of 7–11 yr, and a separate set of filters were used to produce smooth null continuum (9–15 yr for the instrumental series and 59–85 yr for the reconstruction). The 95% confidence intervals for each periodogram were calculated through the chi-squared distribution. Spectral coherence analysis (Percival and Constantine 2006) was performed to test the agreement between the reconstruction and instrumental data across the frequency spectrum. The similarity of each periodogram was compared with standard Gaussian noise using bootstrap simulations ($n = 1000$). In addition, the same coherence analysis was done between the instrumental heavy and nonheavy precipitation totals for the 1949–2004 calibration period.

The precipitation signal detected in these blue oak chronologies is compared with the precipitation response of all available chronologies of total ring width near the study area (i.e., between 37° and 41°N in California). All conifer ($n = 37$) and blue oak ($n = 19$) chronologies were correlated with water year precipitation totals, heavy totals (≥25.4 mm), and nonheavy totals (<25.4 mm) for the period from 1949 to 1978 in common with all tree ring chronologies and the CPC instrumental observations. These correlations highlight the unique and very strong signal of heavy precipitation in selected blue oak chronologies.

3. Results

The instrumental precipitation time series for heavy and nonheavy daily totals during the water year (i.e., ≥25.4 and <25.4 mm) are plotted for the northern California study area in Fig. 1 along with the full water year totals. One inch or 25.4 mm of precipitation represents the 95.4th percentile of the daily totals for the study area (the 95th percentile is 24.20 mm). The 56-yr mean for the CPC regional average is

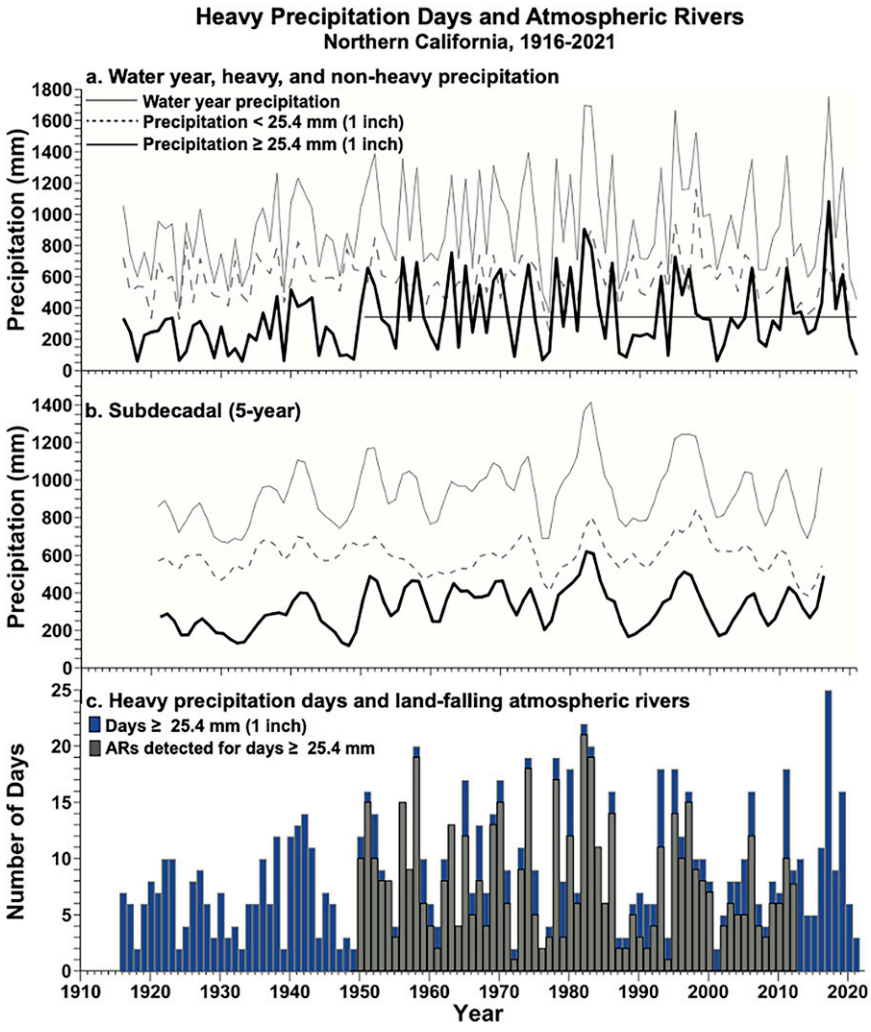

FIG. 1. (a) Heavy daily precipitation ≥ 25.4 mm (i.e., 1 in.; black) and nonheavy precipitation < 25.4 mm (dashed gray) totals for the water year, along with the full water year totals (gray) from 1916 to 2021 for the study area in northern California (see Fig. 2a, below, for location). The three time series were calculated using the CPC unified gauge-based dataset from 1949 to 2021. The same three quantities calculated from the Livneh et al. (2013) dataset are included from 1916 to 1948. The mean is plotted for the CPC heavy totals. Note that heavy precipitation (CPC) is equal to approximately 39% of the water year total in the study area, and the heavy fraction is much more variable than the nonheavy totals. (b) The subdecadal smoothed versions of the water year (gray), heavy (black), and nonheavy (dashed gray) precipitation time series, illustrating that the higher subdecadal variability in the extremes dominates the water year totals. (c) The number of days each year with ≥25.4 mm of precipitation (blue) using the CPC (1949–2021) and the Livneh datasets (1916–48) for the study area. The mean and 80-/20th-percentile thresholds for the CPC data are 10, 16, and 5 days, respectively, for 1949–2021. The atmospheric river chronology at the California coastline is also plotted (1949–2012; gray).

386 mm (15 in.) for the heavy fraction (≥25.4 mm), 589 mm for the nonheavy fraction (23 in.), and 976 mm (38 in.) for the water year total (October–September, 1949–2021). The daily precipitation totals above 25.4 mm only constitute 39% of the water year totals in the study area (61% for the <25.4 mm fraction), but the variance of the heavy daily totals is much higher than for the nonheavy totals (Fig. 1a), as noted for the Delta Catchment by Dettinger et al. (2016). Most of this heavy precipitation (76%) occurred during atmospheric river conditions [i.e., AR days near the Golden Gate identified when any one of four daily measurements met the AR criteria in Rutz et al. (2014)]. The major subdecadal droughts of the 1940s (illustrated using the Livneh data) and 1980s were much more pronounced in the heavy

daily totals, highlighting the importance of a few heavy precipitation events to water supply in California. The daily totals in the upper 5th percentile also represented a larger fraction of the water year precipitation totals during the wet episodes of the early 1980s and 1990s (i.e., 49% and 43%, respectively; Fig. 1b).

The regional blue oak chronology is very highly correlated with water year precipitation totals in the northern California study area at $r = 0.84$ (1949–2004) but is also well correlated with precipitation totaled for just the wettest days each water year (i.e., $r = 0.82$ for daily totals ≥ 25.4 mm). The blue oak correlation with precipitation totaled for all remaining days drops to $r = 0.55$ (the daily totals < 25.4 mm), even though this nonheavy fraction averages 61% of the water year total. These results confirm that blue oak ring-width chronologies constitute exceptionally strong proxies of water year precipitation in California, but also that some blue oak chronologies are equally well correlated with just the heavy daily totals (i.e., correlations of 0.84 vs 0.82, respectively).

The number of days each year with heavy and extreme precipitation ≥25.4 mm is plotted in Fig. 1c using both the Livneh (1916–48) and CPC datasets (1949–2021). On average, there were 10 days each water year with at least 25.4 mm of recorded precipitation in the study area. Just two days above that threshold were recorded in 1949, 1972, and 2001, but 25 days were recorded in 2017. The number of heavy daily totals (Fig. 1c) is highly correlated with the instrumental sum of heavy precipitation above the 25.4-mm threshold ($r = 0.96$; 1949–2021) and with the regional blue oak chronology ($r = 0.79$; 1949–2004). The number of heavy precipitation days and the blue oak chronology are also highly correlated with a time series of atmospheric rivers detected near the study area [$r = 0.92$ and 0.72, respectively, for the count of AR days recorded at 37.5°N, 122.33°W, for 1949–2012 and 1949–2003, when AR conditions were detected for any one of four daily time steps, using Rutz et al. (2014); Fig. 1c].

For a spatial perspective on these precipitation signals, instrumental heavy precipitation totals for the study area were correlated with precipitation summed at each grid point over the western United States on the same days when heavy precipitation was observed in the northern California study region (Fig. 2a). Nonheavy (Fig. 2b) and water year precipitation totals (Fig. 2c) in the study area were also correlated with gridded precipitation sums on the corresponding nonheavy and water year days, again using the same days defined for northern California. Heavy precipitation averaged for the study area is of course well correlated with gridded heavy precipitation nearby, but strong and significant correlations extend across most of the western United States (Fig. 2a). Nonheavy precipitation is well correlated near the study area, but the large-scale West-wide correlations are much weaker (Fig. 2b), as are the large-scale correlations of water year precipitation totals (Fig. 2c). These results indicate that heavy precipitation totals, which are usually associated with landfalling ARs, have a major influence on the climatological pattern of precipitation in the West.

The regional blue oak chronology is also well correlated with gridded precipitation in the West summed on the days identified in the study area with heavy daily totals (Fig. 2d). The highest correlations are observed in the immediate vicinity of the tree-ring chronologies and at higher elevations in the Coast Ranges and Sierra Nevada (Fig. 2d), where precipitation and runoff amounts are usually higher (Kahrl et al. 1979). However, similar to the instrumental data (Fig. 2a), the spatial correlations of blue oak with precipitation on the days in the study area with heavy and extreme totals are strong and significant across most of the western United States (Fig. 2d) and the correlations with precipitation summed for the nonheavy days are much weaker and more regional (Fig. 2e). These selected blue oak chronologies therefore appear to provide useful proxies of temporal and spatial variability of heavy precipitation in the West. Because ARs dictate much of the variance in precipitation extremes, selected blue oak chronologies may also provide insight into past AR activity.

The strong correlation between heavy precipitation totals in northern California and atmospheric rivers is illustrated in Fig. 3a where precipitation totals ≥ 25.4 mm summed for the study area are correlated with the number of ARs observed on those same heavy days on a gridded basis across the West. Correlations exceed 0.90 over most of northern California and are above 0.95 for a small domain inland of Monterey Bay (Fig. 3a). The correlation between nonheavy precipitation totals and AR count at all grid points across the West on the same days associated with nonheavy precipitation in the study area is mapped in Fig. 3b, indicating that ARs play a relatively minor role during days of nonextreme precipitation.

The correlation between the regional blue oak chronology and the count of ARs observed at each grid location on the specific days of heavy precipitation each year in the northern California study area are also very strong and reproduce the spatial pattern seen with the instrumental data (Fig. 3c versus Fig. 3a). Blue oak is not well correlated with AR count over the West on days when nonheavy precipitation occurs in the study area (Fig. 3d), similar to the instrumental data (Fig. 3b). The results in Figs. 2 and 3 demonstrate that the interannual variability of the regional blue oak chronology has a strong temporal and spatial correlation with heavy precipitation totals and atmospheric river activity over California and the western United States, but a much weaker association with nonheavy precipitation totals. An example of this AR signal in blue oak growth can be illustrated with a photomicrograph of annual rings from Mount Diablo and the count of landfalling ARs near the Golden Gate from Rutz et al. (2014). Strong proportionality between AR count and blue oak ring width is apparent (Fig. 3e), even though this is only one tree out of the 140 exactly dated oak trees used to compute the regional chronology. More ARs were observed during wet years of above average growth, and fewer were counted during the below average growth of dry years.

Because of the strong intercorrelation among these precipitation and tree growth variables it is possible to use the ring width chronology to reconstruct heavy daily precipitation amounts ≥ 25.4 mm and the number of days with heavy precipitation each year. The regional blue oak chronology explains 70% of the variance in the transformed heavy precipitation

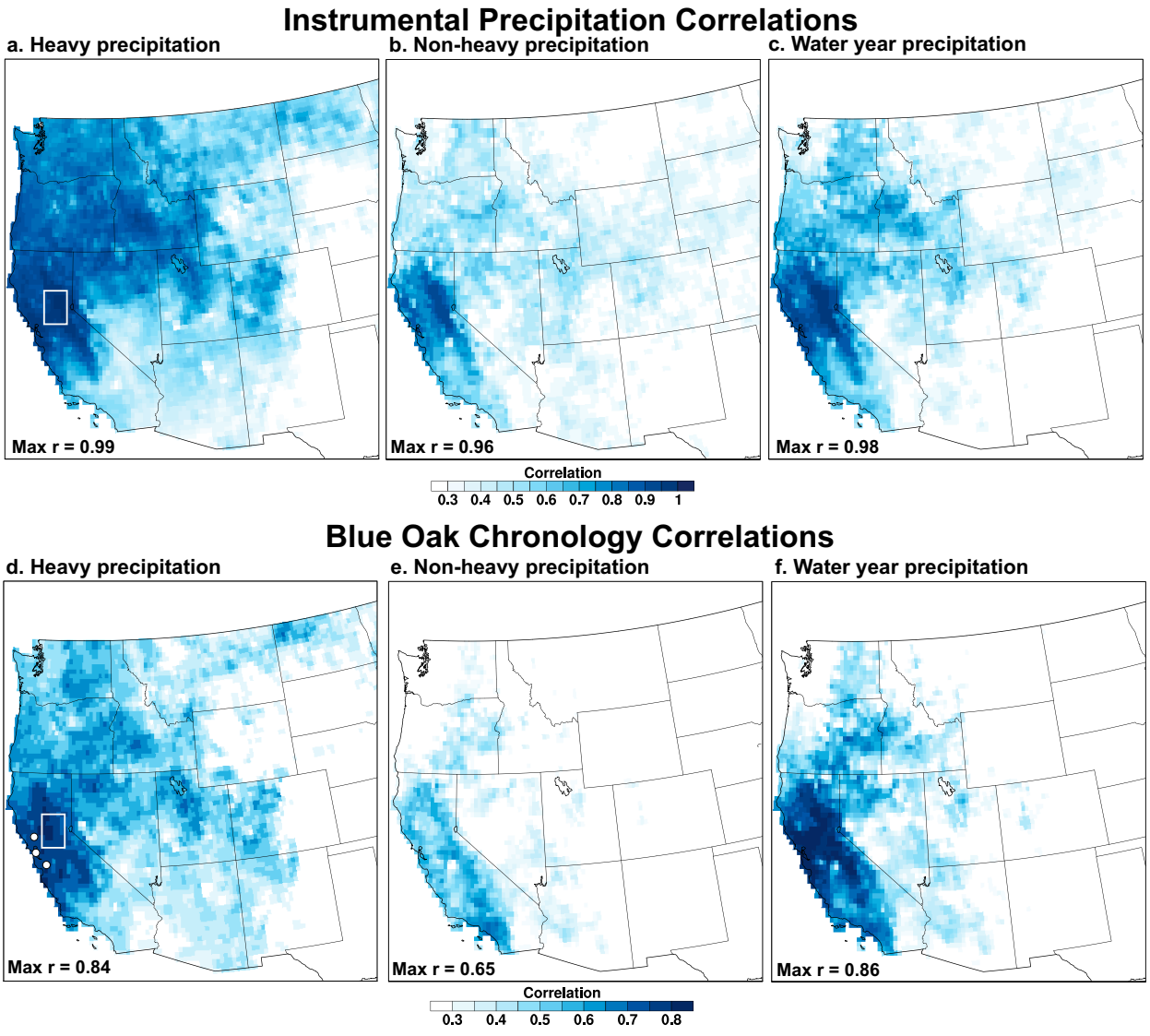

FIG. 2. (a) Heavy instrumental precipitation totals averaged for the study area (white box) were correlated with precipitation summed at each grid point over the West on the same days when heavy precipitation was observed in northern California (an average of 10 days per year). (b) Nonheavy and (c) water year precipitation totals in the study area were also correlated with gridded precipitation sums on the corresponding nonheavy and water year days, also defined for northern California. The regional blue oak chronology was correlated with (d) gridded heavy, (e) nonheavy, and (f) water year precipitation totals as defined in (a)–(c), respectively. The three blue oak sites used for the regional chronology were Pacheco Pass, Mount Diablo, and Putah Creek [white dots in (d), from south to north). The gridded correlations were computed for the 1949–2004 interval in common to the tree ring and precipitation data ($p < 0.05$ for all mapped correlations; the maximum grid point correlation is also noted for each panel).

totals in the northern California study area from 1949 to 2004 (adjusted $R^2 = 0.70$). There is no significant autocorrelation or linear trend in the regression residuals when compared with the square root–transformed instrumental precipitation data (1949–2004), and the estimates are fairly symmetrical around the fitted model (Fig. 4a). The back-transformed final reconstruction is also highly correlated with the instrumental CPC heavy precipitation totals ($r = 0.82$; Figs. 4b and 5a), although the scatter about the regression line increases for the above average estimates, especially for 1952 and 1998, which are overestimated (Figs. 4a,b). The split-period calibration and validation experiments indicate that the reconstruction of heavy precipitation derived from the blue oak chronology strongly validates when compared with independent instrumental observations, with little loss of common variance (Table 1). The full common interval between the CPC and tree-ring data was therefore used to calibrate the final reconstruction (Fig. 5a).

The reconstruction of heavy precipitation was also used to estimate the number of days each year with precipitation ≥ 25.4 mm (Fig. 5b). No data transformation was needed for

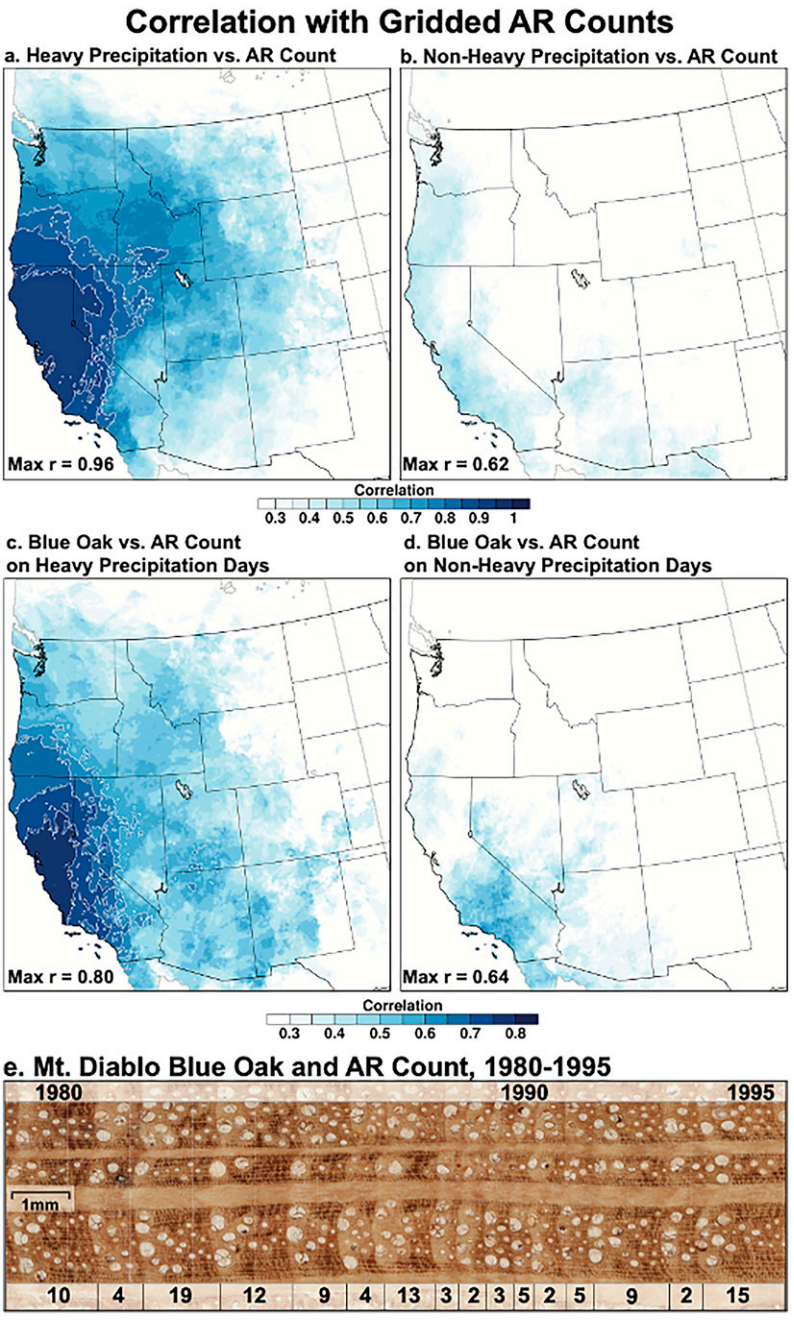

FIG. 3. (a) Instrumental heavy precipitation was correlated with gridded AR counts (Gershunov et al. 2017) on the specific days each year when heavy precipitation (≥25.4 mm) was measured for the study area in northern California. These days of heavy precipitation vary from 2 to 28 days (1949 and 2017, respectively). (b) Nonheavy precipitation was also correlated with gridded AR counts on the corresponding nonheavy days also defined for northern California. The regional blue oak chronology was correlated with gridded AR count on the days with (c) heavy and (d) nonheavy precipitation in the study area [$p < 0.05$ for all correlations mapped; for 1949–2004, with contour intervals plotted above 0.80 in (a) and above 0.60 in (c)]. Note the area of highest correlations (>0.95) near Monterey Bay in (a). (e) A photomicrograph of ring porous annual rings in blue oak from Mount Diablo is reproduced for 1980–95 along with the count of landfalling ARs near the Golden Gate to illustrate the proportionality between oak growth and AR-delivered heavy precipitation. The annual rings are oriented vertically, and two medullary rays run horizontally through the ring sequence.

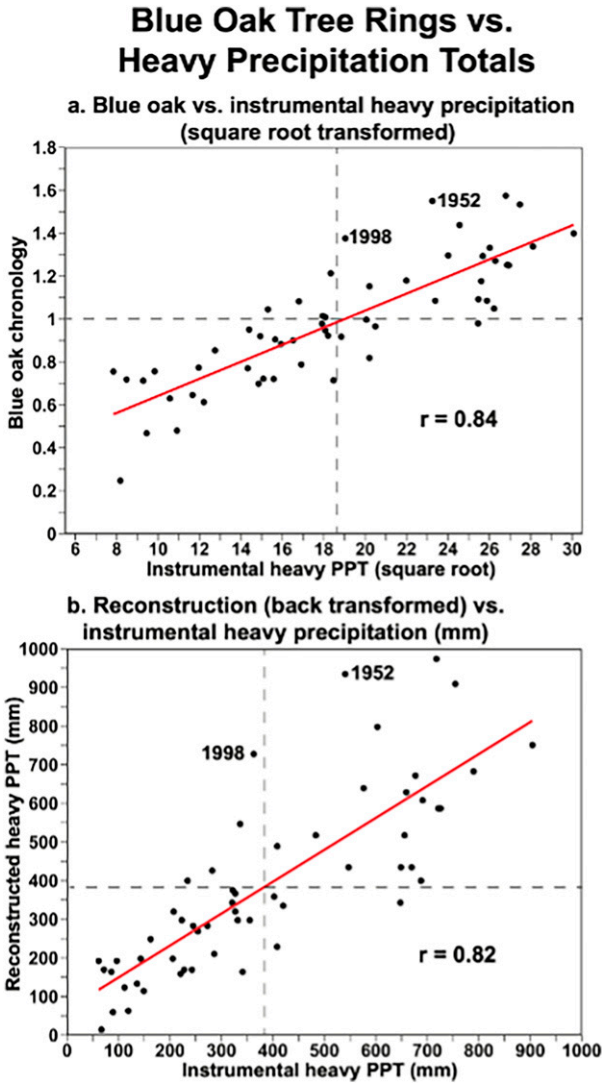

FIG. 4. (a) Scatterplot comparing the blue oak chronology with square root–transformed heavy precipitation totals for the calibration period, 1949–2004. The two largest positive residuals are noted (1952 and 1998) along with the correlation. (b) As in (a), but comparing the back-transformed heavy precipitation reconstruction and the instrumental heavy precipitation totals (mm).

the reconstruction of the number of days with heavy precipitation, and the same full and split-period calibration/validation methods were used (Table 1; note that the assumptions of linear regression were met, and that Poisson regression of heavy precipitation days produced similar estimates). The relationship between the reconstruction and the number of days with heavy precipitation is weaker than with the sum of heavy precipitation, but still explains 59% of the variance in the instrumental number-of-days time series from 1949 to 2004. This number of heavy days reconstruction is also interesting because ARs were detected on approximately 74% of those heavy days based on comparisons between the instrumental data from 1949 to 2012 (Fig. 1c). Presumably, ARs also dominated the reconstructed days of heavy precipitation in the preinstrumental era, particularly for above average days when ARs were detected more frequently in the instrumental data (i.e., ARs on 75% of days with precipitation ≥ 80th percentile vs 61% of days with precipitation ≤ 20th percentile).

Reconstructed heavy precipitation is plotted each year from 1582 to 2021 (including the instrumental observations from 2005 to 2021) along with a smoothed version highlighting subdecadal variability (computed with a 5-yr smoothing spline; Fig. 5a). As noted, the instrumental measurements of heavy precipitation are very well correlated with the back-transformed final reconstruction from 1949 to 2004 (Figs. 4b and 5a). The heavy precipitation totals recorded in the CPC data in 2017 (1080 mm) were nearly equaled or exceeded only six times in the ring width reconstructions (i.e., 1656, 1672, 1730, 1784, 1868, and 1941; Fig. 5a). However, the reconstruction indicates decadal to multidecadal episodes when extreme precipitation surged, both in the amount (Fig. 5a) and the total number of days of heavy precipitation each year (Fig. 5b), most notably during the mid- and late eighteenth century. The closest counterpart to these reconstructed episodes with heavy precipitation totals in the instrumental CPC data from 1949 to 2021 may be the period from 1978 to 1986 (Figs. 1a,c). Because this episode of heavy precipitation in the early 1980s was associated with frequent atmospheric rivers (Fig. 1c) it is likely that the reconstructed episodes of heavy precipitation days and totals in the 18th century were also associated with an increase in the frequency and/or intensity of landfalling ARs in northern California.

The 1940s may represent another analog for the episodes of heavy precipitation in the eighteenth century based on the tree-ring reconstructions (Figs. 5a,b). The Livneh et al. (2013) estimates for the study area (Fig. 1a) do not appear to match the intensity of the tree-ring reconstructed values during the late 1930s and early 1940s (Figs. 5a,c), but they were elevated well above the mean for the period 1916–48 (Figs. 1a,c). The heavy precipitation in northern California during 2017 (California DWR 2017) was exceptional even when compared with the last 440 years (instrumental observations are appended to the reconstruction in Fig. 5a, which ends in 2004), but it was the singular wet extreme during the dry interval when heavy precipitation was below the mean for 16 of 19 years (1998–2016).

The year 1862 is reconstructed to have been in the upper 5th percentile of all years from 1582 to 2004 but that may not be a sufficiently extreme estimate because 1861–62 was one of the heaviest water years of precipitation in California history, and certainly among the wettest in terms of flooding (Dettinger and Ingram 2013) when most of the Central Valley flooded (McGlashan and Briggs 1939; Moftakhari et al. 2013). Drought preceded 1862 (smooth curve in Fig. 5a), most notably the severe sustained 5-yr drought reconstructed from 1855 to 1859 (1860 and 1861 were slightly above average; Figs. 5a,b). These dry conditions prior to 1862 may have reduced to stored food reserves in blue oak trees, limiting their ability to respond to the extreme precipitation of 1862. Some of the precipitation in 1862 no doubt failed to infiltrate soils and ran off, thus contributing to the underestimation from the tree rings. In contrast, 1868 was also one of the years of heaviest precipitation in

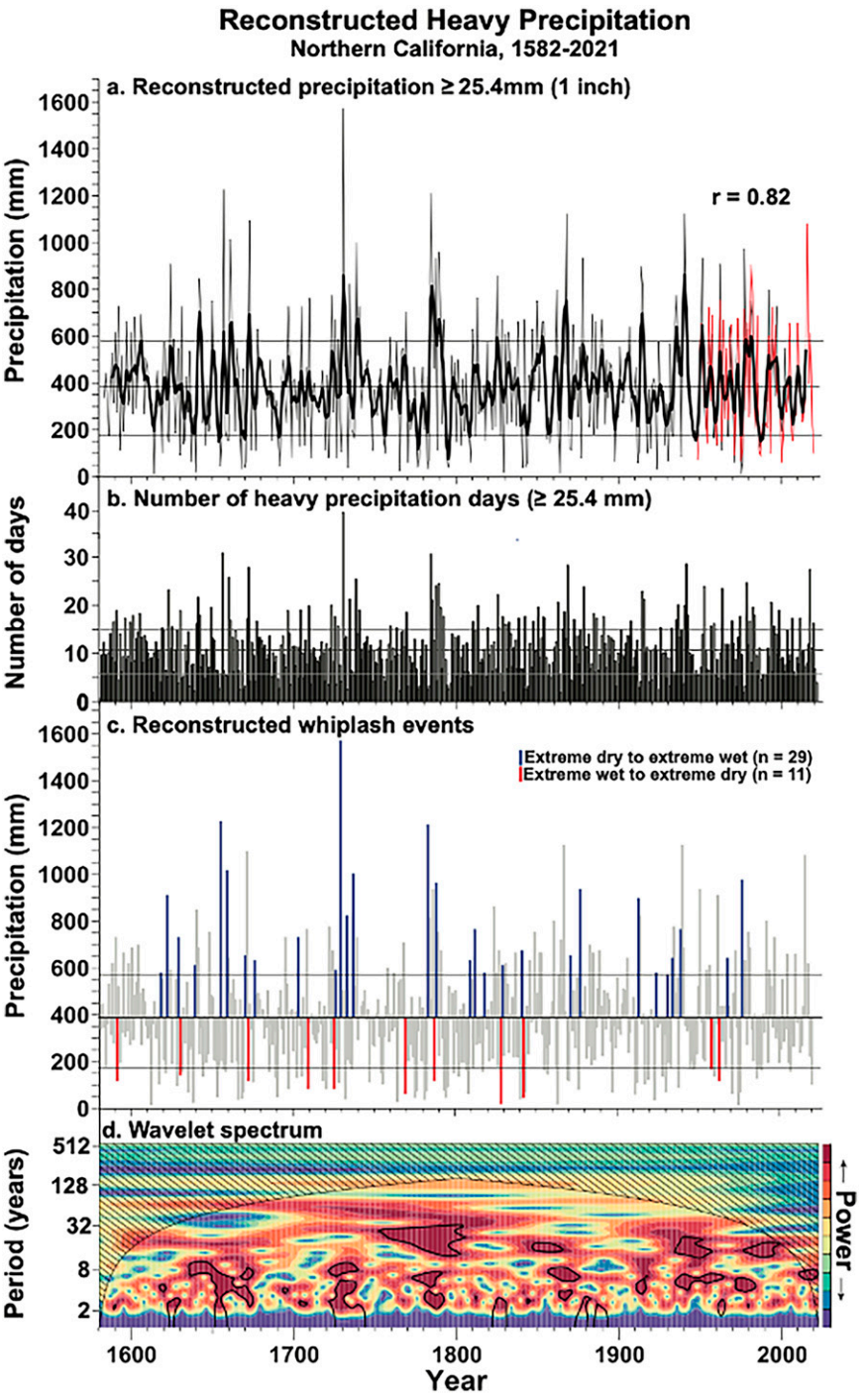

FIG. 5. (a) The tree-ring reconstruction of heavy precipitation totals in the northern California study area (gray) along with the subdecadal smooth values (black) and the heavy instrumental totals (red). The reconstruction extends from 1582 to 2004, and the CPC instrumental observations are appended from 2005 to 2021. The mean and upper and lower 20th percentiles computed for the full period 1582–2021 are also plotted. The reconstruction and instrumental values are correlated from 1949 to 2004 at $r = 0.82$. (b) Reconstructed heavy precipitation was used to estimate the number of days each year with heavy precipitation. The reconstructed values extend from 1582 to 2004, and the instrumental count was appended from 2005 to 2021. The mean and the upper and lower 20th percentile thresholds are also plotted. (c) Abrupt 1-yr changes from dry-to-wet (blue bars) or wet-to-dry extremes (red bars) are plotted on the heavy precipitation reconstruction (gray bars) using the upper and lower 20th-percentile thresholds to define these extreme whiplash events. (d) The wavelet spectrum for the reconstruction of heavy precipitation totals (1582–2021). The black contour line identifies significant spectral power ($p < 0.05$).

TABLE 1. Calibration and validation statistics for the tree-ring reconstruction of heavy precipitation amounts and the number of heavy precipitation days each year from 1582 to 2021. Two additional reconstructions were calibrated for total precipitation over the water year (October–September), and the nonheavy precipitation totaled for days with <25.4 mm over the water year for comparison with the reconstruction of heavy precipitation amounts. The instrumental precipitation data for the northern California study area were square root transformed prior to calibration and validation (R^2 adj = explained variance adjusted for the loss of one degree of freedom; r = Pearson correlation coefficient; RE = reduction of error; CE = coefficient of efficiency; Fritts 1976).

	Calibration			Verification		
Variable	Period	r	R^2 adj	Period	r	RE/CE
$\sqrt{\text{Heavy precipitation}}$	1949–2004	0.84	0.70	1949–2004	—	—
	1977–2004	0.82	0.67	1949–76	0.87	0.70/0.70
	1949–76	0.87	0.75	1977–2004	0.82	0.63/0.63
	Transfer function: $\sqrt{\hat{y}} = 1.141 + 17.766X_t$					
Heavy precipitation days	1949–2004	0.77	0.59	1949–2004	—	—
	1977–2004	0.79	0.62	1949–76	0.76	0.56/0.55
	1949–76	0.76	0.58	1977–2004	0.79	0.48/0.46
Water year	1949–2004	0.84	0.71	—	—	—
Nonheavy precipitation	1949–2004	0.55	0.29	—	—	—

California history (McGlashan and Briggs 1939) and is well represented in the reconstruction as the sixth-wettest year since 1582 (Fig. 5a). The differences between the reconstruction for 1862 and 1868 illustrate some of the uncertainty involved in using biological proxies to estimate heavy precipitation. The heavy precipitation of 1868 was preceded by three years of above average precipitation (Fig. 5a), which may have improved stored photosynthate in oaks, facilitating the growth response to the precipitation extremes of 1868. If antecedent drought or wetness do indeed impact the fidelity of heavy precipitation estimates from blue oak in a systematic manner, it may be possible to empirically model these effects on comparison with instrumental precipitation data and develop adjustment factors to enhance the regression-based estimates of heavy precipitation. The development of additional blue oak chronologies based on a variety of age classes and site types may also lead to improved estimation of extremes.

The abrupt reversal of precipitation from the drought of 2012–16 to the extreme heavy precipitation of 2017 is a feature of California's highly variable Mediterranean climate and this volatility is projected to increase in the coming decades with anthropogenic forcing even without a large change in mean precipitation (Polade et al. 2014; Swain et al. 2018). Despite uncertainty in the estimation of extremes, the blue oak reconstruction can provide a useful historical perspective on the volatility of heavy precipitation in northern California. Figure 5c identifies the years of abrupt change from dry to wet extremes, or the opposite, using the 20th- and 80th-percentile thresholds to define extremes (i.e., "whiplash" events). The reconstructions indicate that there were 29 dry-to-wet whiplash events from 1582 to 2004, but only 11 large wet-to-dry reversals (Fig. 5c). The ratio of whiplash types in the reconstruction may be sensitive to the distribution of the residuals computed for the reconstruction of heavy precipitation (see Wahl et al. 2020). Nonetheless, there were four dry-to-wet and only two wet-to-dry whiplash events in the instrumental data from 1949 to 2021 (not shown).

The reconstruction does not indicate any recent increase in whiplash events, but decadal surges in heavy precipitation amount and volatility have occurred prior to the instrumental record, most notably during the 1720–40s and 1780s (Fig. 5c). These surges may not be randomly distributed through time, because 10–20-yr-long intervals without heavy precipitation extremes or volatility are also reconstructed. Volatility is expected to increase in the future (Polade et al. 2014; Gershunov et al. 2019), but the new blue oak reconstructions suggest that decade-long episodes of increased volatility of heavy precipitation may also be a component of natural variability in California.

The dry episodes in the late 1980s and 2000s, when few heavy precipitation events were recorded in the instrumental observations (Figs. 1a,c), are matched by a number of similar dry spells over the past 440 years in the reconstructions (Figs. 5a,b). The irregular occurrence of both decadal wet and dry episodes in reconstructed extremes results in multidecadal intervals of positive and negative trend in heavy precipitation totals (e.g., 1730–80, 1800–70; Fig. 5a), but there is no evidence for any persistent trends of either sign in the instrumental or reconstructed heavy precipitation totals in recent decades. Apart from 2017, there has been no detected increase in the heaviest daily precipitation amounts as projected by some climate models due to anthropogenic forcing for later in this century (see also Lamjiri et al. 2018).

Wavelet analysis (Torrence and Compo 1998) of the reconstructed heavy precipitation totals indicates concentrations of time series variance in the El Niño–Southern Oscillation (ENSO) band from 3 to 8 years, but statistical significance is only episodic over the past 440 years, often during the regimes of elevated frequency and intensity of precipitation extremes (e.g., 1650s, 1730s, 1780s, and 1860s; Fig. 5d). No significant multidecadal wavelet power is detected in the reconstruction. However, the estimate is not suitable for the recovery of low-frequency climate variance, because the reconstruction was detrended to remove long-term growth trend unrelated to climate and autoregressively modeled to remove low-order autocorrelation. This was done to better match the persistence structure of the instrumental heavy precipitation time series with which the tree-ring data were calibrated. Nonetheless,

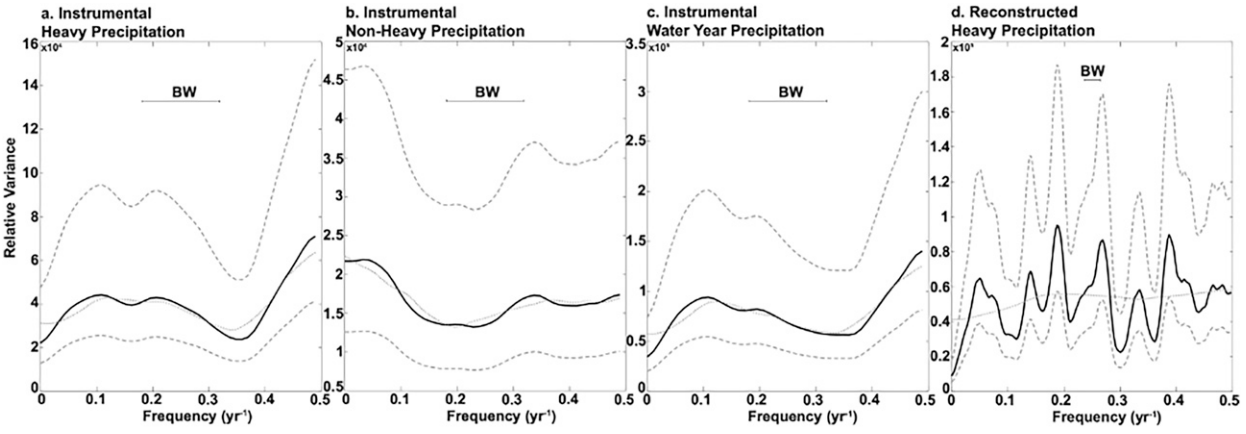

FIG. 6. Smoothed periodograms of instrumental (a) heavy, (b) nonheavy, and (c) water year total precipitation calculated from the discrete Fourier transform of each time series for the period 1949–2021. Smoothing spans for a Daniell filter were equal for all periodograms (7–11 yr) and null continuums (67–82 yr). The length of each bandwidth (BW) is noted. (d) The smoothed periodogram of the reconstruction (1582–2021), with the same smoothing filters as applied to the instrumental data in (a)–(c).

there is some transient wavelet power in the quasi-decadal band centered at approximately 15 years, most significantly in the late-eighteenth and late-twentieth centuries (Fig. 5d).

Separating instrumental daily precipitation data into the heavy and nonheavy totals results in interesting differences in the power spectrum. The heavy precipitation totals are dominated by variance at higher frequencies (periods $\leq$ 3 yr; Fig. 6a) while the nonheavy precipitation fraction has greater power at low frequencies (periods $\geq$10 yr; Fig. 6b). However, because of the low effective sample sizes in these instrumental observations, none of the peaks present in the heavy, nonheavy, and water year spectra are significant. Spectral analysis was also performed using the full 440-yr reconstruction allowing for a better resolution of the frequency spectrum of heavy precipitation (Fig. 6d). The reconstruction exhibits some significant variance at the ENSO and biennial frequencies (i.e., ~5.3 and 2.6 yr), but wavelet analysis indicates that power at these frequencies has been episodic over the past 440 years (Fig. 5d). The nonstationarity of the ENSO signal is an important insight revealed by the tree-ring data and understanding why this signal may be episodic could lead to improved forecasting of heavy precipitation variability. A quasi-decadal variance component has been identified in previous analyses of California precipitation (St. George and Ault 2011; Williams et al. 2021) and landfalling ARs (Stuivenolt-Allen et al. 2021), but these instrumental and blue oak-based reconstruction results suggest that high-frequency variability in the biennial and ENSO bands may dominate heavy precipitation totals and low-frequency decadal power might be concentrated in the nonheavy fraction of precipitation in northern California.

The 440-yr blue oak reconstruction of heavy precipitation explains approximately 70% of the variance in the instrumental extremes and cross-spectral coherency analysis indicates that the reconstruction is in fact coherent with the instrumental observations of heavy precipitation and water year totals across the frequency domain ($p < 0.01$, for 1949–2004; spectrum not shown). The reconstruction is not coherent with nonheavy precipitation totals at frequencies lower than decadal (squared coherence < 0.28 at frequencies $\leq$0.1 yr^{-1}; $p > 0.10$). Instrumental heavy and instrumental nonheavy precipitation are also not coherent at these low frequencies ($p \geq 0.10$ for 1949–2004; not shown). These results indicate that the reconstruction is primarily correspondent with heavy rather than nonheavy precipitation variability and that the agreement between the instrumental and reconstructed heavy precipitation is very strong across all time scales.

In engineering practice, precipitation data are routinely used to estimate return periods or annual probabilities, yielding, for example, estimates of 100-yr storms and floods useful for design and planning purposes. The new reconstructions of heavy-precipitation amounts presented here for northern California offer a unique opportunity to make return-period estimates on a much longer record (Fig. 7). This can help to improve estimates of return periods for the heaviest and most unusual storm totals and provide indications of the extent to which instrumental estimates might be overly dependent on the specific climate of the modern period when direct observations are available. Are the return-period estimates from the instrumental data only reflective of the unique sequence of precipitation events during the twentieth and twenty-first centuries or has the longer-term history of heavy storms been such that our modern return period estimates happened by providence to represent California's heavy precipitation probabilities more generally?

The return probabilities estimated on the instrumental and reconstructed totals are very similar (Fig. 7), despite large natural climate variability, possible recent influences of anthropogenic climate change, and the large difference in the length of the two records. The estimated probabilities of heavy precipitation totals based on the instrumental and reconstructed data are both approximately 350 mm for a 50% recurrence probability, 700 mm for 10%, and 900 mm for a 4% probability (Fig. 7). Return periods are also calculated from the reconstruction for

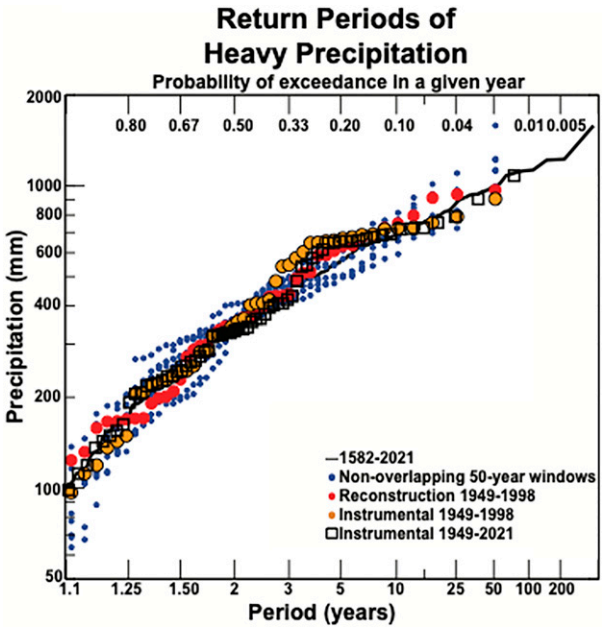

FIG. 7. Return periods and probabilities for the instrumental and reconstruction heavy precipitation totals (daily amounts ≥25.4 mm). The black line connects the discrete return periods computed for the full 440-yr reconstruction (1582–2021), and the blue dots are return periods for nonoverlapping 50-yr intervals in the reconstruction. Instrumental return periods are plotted for 1949–98 (orange circles) and 1949–2021 (squares). Reconstructed return periods restricted to 1949–98 are also plotted for comparison (red circles).

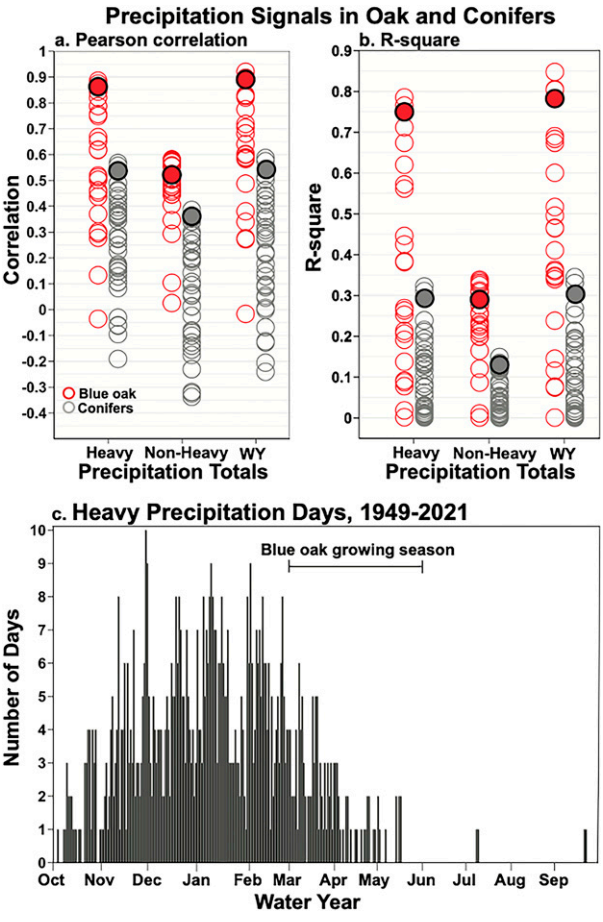

FIG. 8. (a) All available blue oak and conifer chronologies (n = 19 and 37, respectively) in the vicinity of the study area in California (37°–41°N; Fig. 2a) were correlated with heavy, nonheavy, and water year precipitation totals for the common period 1949–78 (the correlation levels are indicated with red for blue oak and gray for the conifer chronologies). The correlations based on the regional blue oak chronology and an average of the three conifer chronologies most highly correlated with heavy precipitation are also plotted (solid red and gray symbols, respectively). (b) As in (a), but the correlations have been squared to estimate common variance with each precipitation variable. Only some blue oak and none of the conifer chronologies appear to provide strong proxies for the heaviest precipitation fraction in the northern California study area. (c) The frequency histogram of the number of days of the water year with heavy precipitation ≥25.4 mm for 1949–2021. The approximate growing season for blue oak is also indicated (i.e., March–May).

nonoverlapping 50-yr intervals and those estimates are all distributed in a compact manner around the recurrence estimates based on the entire reconstruction and the instrumental record (Fig. 7). These surprising results suggest that the distribution of heavy precipitation over the study area has been stable enough during the past 400 years so that the 73-yr-long instrumental time series is generally adequate for the estimation of return probabilities of heavy precipitation totals under natural conditions. Given the practical implications of this conclusion, the estimation of return intervals deserves further testing with an expanded network of blue oak chronologies specifically sensitive to heavy precipitation totals.

To summarize the unique nature of the blue oak proxy for heavy precipitation in California, we correlated all available conifer and blue oak chronologies in the vicinity of the study area (i.e., between 37° and 41°N in California) with the three CPC instrumental precipitation variables: the heavy (≥25.4 m), nonheavy (<25.4 m), and water year totals (Figs. 8a,b). The correlations were computed for the 30-yr interval in common to all tree-ring chronologies and the CPC precipitation data (1949–78). Three important conclusions seem warranted:

1) The correlation between the blue oak chronologies and both heavy and water year precipitation totals are generally much higher than that observed for the conifers.
2) The conifer chronologies are, on average, equally well correlated with heavy and water year precipitation totals (similar to blue oak), likely because of the very strong correlation between these two categories in the instrumental observations.
3) The difference in correlation and common variance fractions between the heavy and nonheavy components of precipitation tends to be much higher for the blue oak chronologies (e.g., R^2 = 0.76 vs 0.27 for the regional blue oak chronology, as compared with R^2 = 0.28 vs 0.11 for an average of the three best conifer chronologies; Figs. 8a,b). This strong

separation of signal between the heavy and nonheavy fractions is evidence for the growth effectiveness of the heaviest precipitation fraction in blue oak.

Because the variability of water year precipitation in California is so strongly driven by the extremes and selected blue oak chronologies are uniquely sensitive to those heavy precipitation totals, the results presented in Fig. 8 indicate that blue oak will be important for improved reconstructions of both heavy and water year precipitation totals. Precipitation reconstructions in northern California based only on conifer ring width chronologies are not likely to be capable of capturing the full range of variability present in the instrumental observations. However, certain native conifer species can be very well correlated with precipitation, including bigcone Douglas-fir (*Pseudotsuga macrocarpa*; Haston and Michaelsen 1997) and subannual conifer chronologies of latewood width in ponderosa pine and Jeffrey pine (*P. ponderosae* and *P. jeffreyi*; Howard et al. 2023). Carefully selected conifer and blue oak chronologies from this region may contribute to long-term estimations of seasonal and storm total precipitation in Southern California.

4. Discussion and conclusions

The registration of heavy precipitation totals in the regional blue oak chronology from northern California is remarkable. The correlation with the sum of the daily totals ≥ 25.4 mm (1 in.) is nearly equal to the correlation with precipitation summed for the entire water year (r = 0.82 vs 0.84; 1949–2004), even though the heavy amounts only represent 39% of the water year totals in the study area. By comparison, the correlation between the blue oak chronology and the sum of precipitation for all remaining days of the year (≤25.4 mm day^{-1}) is only r = 0.55. Therefore, the proxy climate signal in these selected blue oak chronologies from California, which are in fact among the most precipitation sensitive tree-ring chronologies currently available (St. George and Ault 2014), turns out to be the sum of the few very wet days each year receiving at least 1 in. of precipitation. These few days of heavy precipitation are crucial to water supply and flood risk in California and most heavy precipitation occurs during atmospheric river conditions (Dettinger and Cayan 2014). The reconstructions presented in Fig. 5 represent well-calibrated and independently validated estimates of both heavy precipitation totals and the number of days with heavy precipitation each year, based on selected blue oak chronologies especially sensitive to heavy precipitation.

The near equivalence of correlation when the blue oak chronology is compared with the heavy precipitation fraction and the full water year precipitation total appears to be primarily due to the nature of California precipitation where the extremes dictate the bulk of variance in the water year totals. But the results presented here also suggest that a degree of direct physical forcing may also be involved in the heaviest precipitation events and blue oak growth. Together, the various factors in the blue oak response to heavy precipitation appear to include:

1) As noted, heavy precipitation totals are very highly correlated with water year totals in the instrumental measurements for the northern California study area at interannual and decadal time scales (r = 0.90 and 0.89, respectively; 1949–2021). However, instrumental water year precipitation is correlated with the nonheavy precipitation totals more highly than the blue oak chronology (r = 0.77 vs 0.55, respectively), indicating some true discrimination between the heavy and nonheavy fractions in the proxy.
2) Heavy precipitation in California most often occurs during atmospheric river conditions, but ARs are less common during nonheavy precipitation events. ARs can bring more steady, soaking, and widespread precipitation in comparison with other systems and may therefore deliver much of the soil moisture and tree growth effective precipitation in California.
3) Heavy precipitation totals, the approximate upper 5th percentile of days with precipitation, may be more effective at filling the soil moisture column and thereby favoring blue oak growth, more so than the nonheavy fraction, some of which is subject to evaporation or sublimation before enhancing soil moisture and tree growth. Because there is often separation between the arrival of heavy precipitation and the blue oak growing season (Fig. 8c), we suspect that the deep percolation of precipitation into the subsoil during the extremes tends to buffer that moisture from evaporation, making it available to the oaks at some low elevation sites once the growing season begins in February or March. The nonheavy precipitation fraction will mostly wet the shallow soil, and thus may be more vulnerable to evaporative loss, thereby shifting blue oak moisture dependence toward the heavy precipitation fraction.
4) Blue oak woodlands are found at lower and warmer elevations of the Coast Ranges and Sierra Nevada where precipitation most frequently occurs as rain rather than snow (Kahrl et al. 1979). Consequently, the nonheavy fraction does not tend to be stored as snow on the blue oak landscape that can subsequently melt into the soil column to enhance tree growth later in the calendar year and thereby diminish the response to just the heaviest precipitation events. By contrast, conifers growing at higher cooler altitudes more often depend on annual precipitation accumulated in the seasonal snowpack. The total amount of water in the snowpack by the time it melts and releases water to the soil or runoff is the sum of water from the heavy and nonheavy precipitation fractions. Consequently, the distinction between those two precipitation fractions appears to be less apparent for mid- to higher-elevation conifers.
5) The growing season for blue oak, especially those near the lower forest border, typically occurs from late February into late May (Fig. 8c; Burns and Honkala 1990). This season of annual ring formation overlaps the latter portion of the wet season when soil moisture may be filled by heavy early wet season storms antecedent to growth and by late season storms concurrent with growth (Fig. 8c). However, deciduous blue oak may flush new leaves following very wet events in midwinter (Haggerty 1994) or even retain

some leaves through the entire winter under moist conditions (Pavlik et al. 1991), both allowing for photosynthesis under favorable conditions during the heart of the wet season. These are important distinctions when compared with many conifer species in colder mid- to higher-elevation forests in California where growth does not begin before May (Burns and Honkala 1990) on locations that benefit from snowpack recharge of soil moisture in late spring and early summer. In addition, the melting snowpack in the conifer zone may not deliver moisture to the subsoil quite as effectively as heavy rainfall events in the lower-elevation blue oak zone.

The blue oak ring width chronology calibrates 70% of the variance in the square root transformed time series of instrumental heavy precipitation totals, and the back-transformed reconstruction is correlated with the original untransformed heavy precipitation series at $r = 0.82$ (1949–2004; Figs. 4b and 5a). Some of the over- and underestimation error in the reconstruction is likely to arise from two principal issues: First, on days with extremely heavy precipitation when the infiltration rate is exceeded or the soil has reached field capacity, any excess precipitation will run off and be unable to benefit tree growth. This could lead to an underestimation of heavy precipitation totals based on the ring width chronology. Second, because a threshold is being used to define "heavy precipitation" (≥25.4 mm), daily precipitation amounts near but below the threshold may also enhance soil moisture and tree growth, potentially leading to an overestimation of precipitation in the heavy fraction based on the ring width chronology. The two largest overestimations were reconstructed in 1952 and 1998 (Figs. 4a,b) when precipitation just below the heavy threshold constituted an unusually large fraction of the annual total (both years had at least 10 days of precipitation between 19.05 and 25.4 mm).

Fortunately, the blue oak chronology is very highly correlated with precipitation and especially heavy precipitation, so the uncertainty inherent in the reconstructions is relatively low. It should be possible to increase the fidelity of the reconstructions of heavy precipitation while reducing the uncertainty with the development of additional moisture sensitive blue oak chronologies. The correlations with heavy and nonheavy precipitation indicate that there may be site types within the blue oak woodlands of northern California that are uniquely sensitive to heavy precipitation (Fig. 8a). Preliminary correlation analyses (not shown) indicate that this may also be true among the various ring width chronologies of blue oak in Southern California. Identifying and sampling the most sensitive site types could lead to improved estimation of heavy precipitation totals in California over the past 500 years.

Acknowledgments. This research was sponsored by the California Department of Water Resources (4600013361). We acknowledge the assistance and suggestions of Daniela Granato-Souza, Daniel Griffin, Cary Mock, and two anonymous reviewers of the paper. CPC and Livneh data were provided by the NOAA/ESRL/ Physical Sciences Laboratory (https://psl.noaa.gov/data/gridded/index.html).

Data availability statement. Upon publication, the data developed for this article will be available from the authors and will be contributed to the International Tree-Ring Data Bank at the NOAA Paleoclimatology Program (https://www.ncdc.noaa.gov/dataaccess/paleoclimatology-data).

REFERENCES

Bloomfield, P., 2000: *Fourier Analysis of Time Series: An Introduction*. 2nd ed. John Wiley and Sons, 261 pp.

Borkotoky, S. S., A. P. Williams, E. R. Cook, and S. Steinschneider, 2021: Reconstructing extreme precipitation in the Sacramento River watershed using tree-ring based proxies of cold-season precipitation. *Water Resour. Res.*, **57**, e2020WR028824, https://doi.org/10.1029/2020WR028824.

Burns, R. M., and B. H. Honkala, 1990: Silvics of North America: 1. Conifers; 2. Hardwoods. Agriculture Handbook 654, Forest Service, U.S. Department of Agriculture, 877 pp., https://www.srs.fs.usda.gov/pubs/misc/ag_654/table_of_contents.htm.

California DWR, 2017: Water Year 2017. Hydroclimate Rep., California Dept. of Water Resources, 32 pp., https://water.ca.gov/-/media/DWR-Website/Web-Pages/Programs/Flood-Management/Flood-Data/Climate-summaries/Hydroclimate_Report_2017-ADA-Final.pdf.

Cook, E. R., and P. J. Krusic, 2005: Program ARSTAN: A tree-ring standardization program based on detrending and autoregressive time series modeling, with interactive graphics. Tree-Ring Laboratory of Lamont–Doherty Earth Observatory Doc., 14 pp., https://www.ltrr.arizona.edu/~sheppard/presession/arsreadme_135.doc.

——, ——, K. Peters, and R. L. Holmes, 2017: Program ARSTAN (version ARSTAN 49v1a), Autoregressive Tree-Ring Standardization Program. Tree-Ring Laboratory of Lamont–Doherty Earth Observatory, https://www.ldeo.columbia.edu/tree-ring-laboratory/resources/software; https://www.geog.cam.ac.uk/research/projects/dendrosoftware/.

Corringham, T. W., F. M. Ralph, A. Gershunov, D. R. Cayan, and C. A. Talbot, 2019: Atmospheric rivers drive flood damages in the western United States. *Sci. Adv.*, **5**, eaax4631, https://doi.org/10.1126/sciadv.aax4631.

Dettinger, M. D., 2013: Atmospheric rivers as drought busters on the U.S. West Coast. *J. Hydrometeor.*, **14**, 1721–1732, https://doi.org/10.1175/JHM-D-13-02.1.

——, and B. L. Ingram, 2013: The coming megafloods. *Sci. Amer.*, **308**, 64–71, https://doi.org/10.1038/scientificamerican0113-64.

——, and D. R. Cayan, 2014: Drought and the California delta—A matter of extremes. *San Francisco Estuary Watershed Sci.*, **12**, 4, https://doi.org/10.15447/sfews.2014v12iss2art4.

——, F. M. Ralph, T. Das, P. J. Neiman, and D. Cayan, 2011: Atmospheric rivers, floods, and water resources of California. *Water*, **3**, 445–478, https://doi.org/10.3390/w3020445.

——, J. Anderson, M. L. Anderson, L. R. Brown, D. R. Cayan, and E. Maurer, 2016: Climate change and the delta. *San Francisco Estuary Watershed Sci.*, **14**, 5, https://doi.org/10.15447/sfews.2016v14iss2art5.

Fritts, H. C., 1976: *Tree Rings and Climate*. Academic Press, 582 pp.

Gao, Y., J. Lu, L. R. Leung, Q. Yang, S. Hagos, and Y. Qian, 2015: Dynamical and thermodynamical modulations on future changes of landfalling atmospheric rivers over western North America. *Geophys. Res. Lett.*, **42**, 7179–7186, https://doi.org/10.1002/2015GL065435.

Gershunov, A., T. Shulgina, F. M. Ralph, D. A. Lavers, and J. Rutz, 2017: Assessing the climate-scale variability of atmospheric rivers affecting western North America. *Geophys. Res. Lett.*, **44**, 7900–7908, https://doi.org/10.1002/2017GL074175.

——, and Coauthors, 2019: Precipitation regime change in western North America: The role of atmospheric rivers. *Sci. Rep.*, **9**, 9944, https://doi.org/10.1038/s41598-019-46169-w.

Griffin, D., and K. J. Anchukaitis, 2014: How unusual is the 2012–2014 California drought? *Geophys. Res. Lett.*, **41**, 9017–9023, https://doi.org/10.1002/2014GL062433.

Haggerty, P. K., 1994: Damage and recovery in southern Sierra Nevada foothill oak woodland after a severe ground fire. *Madrono*, **41**, 185–198.

Haston, L., and J. Michaelsen, 1997: Spatial and temporal variability of Southern California precipitation over the last 400 yr and relationships to atmospheric circulation patterns. *J. Climate*, **10**, 1836–1852, https://doi.org/10.1175/1520-0442(1997)010<1836:SATVOS>2.0.CO;2.

Higgins, R., W. Shi, E. Yarosh, and R. Joyce, 2000: Improved United States precipitation quality control system and analysis. NCEP/Climate Prediction Center ATLAS No. 7, https://www.cpc.ncep.noaa.gov/research_papers/ncep_cpc_atlas/7/toc.html.

Higgins, R. W., V. B. S. Silva, W. Shi, and J. Larson, 2007: Relationships between climate variability and fluctuations in daily precipitation over the United States. *J. Climate*, **20**, 3561–3579, https://doi.org/10.1175/JCLI4196.1.

Howard, I. M., D. W. Stahle, M. C. A. Torbenson, D. Granato-Souza, and C. Poulsen, 2023: The flood risk and water supply implications of seasonal precipitation reconstructions in northern California. *San Francisco Estuary Watershed Sci.*, in press.

Kahrl, W. L., W. A. Bowen, S. Brand, M. L. Shelton, D. L. Fuller, and D. A. Ryan, 1979: *The California Water Atlas*. Governor's Office of Planning and Research, 118 pp.

Lamjiri, M. A., M. D. Dettinger, F. M. Ralph, N. S. Oakley, and J. J. Rutz, 2018: Hourly analyses of the large storms and atmospheric rivers that provide most of California's precipitation in only 10 to 100 hours per year. *San Francisco Estuary Watershed Sci.*, **16**, 1, https://doi.org/10.15447/sfews.2018v16iss4art1.

Livneh, B., E. A. Rosenberg, C. Lin, B. Nijssen, V. Mishra, K. M. Andreadis, E. P. Maurer, and D. P. Lettenmaier, 2013: A long-term hydrologically based dataset of land surface fluxes and states for the conterminous United States: Update and extensions. *J. Climate*, **26**, 9384–9392, https://doi.org/10.1175/JCLI-D-12-00508.1.

McGlashan, H. D., and R. C. Briggs, 1939: Floods of December 1937 in northern California. USGS Water Supply Paper 843, 497 pp., https://pubs.usgs.gov/wsp/0843/report.pdf.

Meko, D. M., M. D. Therrell, C. H. Baisan, and M. K. Hughes, 2001: Sacramento River flow reconstructed to A.D. 869 from tree rings. *J. Amer. Water Resour. Assoc.*, **37**, 1029–1039, https://doi.org/10.1111/j.1752-1688.2001.tb05530.x.

——, D. W. Stahle, D. Griffin, and T. A. Knight, 2011: Inferring precipitation-anomaly gradients from tree rings. *Quart. Int.*, **235**, 89–100, https://doi.org/10.1016/j.quaint.2010.09.006.

Moftakhari, H. R., D. A. Jay, S. A. Talke, T. Kukulka, and P. D. Bromirski, 2013: A novel approach to flow estimation in tidal rivers. *Water Resour. Res.*, **49**, 4817–4832, https://doi.org/10.1002/wrcr.20363.

Pavlik, B. M., P. C. Muick, S. G. Johnson, and M. Popper, 1991: *Oaks of California*. Cachuma Press, 184 pp.

Percival, D. B., and W. L. B. Constantine, 2006: Exact simulation of Gaussian time series from nonparametric spectral estimates with application to bootstrapping. *Stat. Comput.*, **16**, 25–35, https://doi.org/10.1007/s11222-006-5198-0.

Polade, S. D., D. W. Pierce, D. R. Cayan, A. Gershunov, and M. D. Dettinger, 2014: The key role of dry days in changing regional climate and precipitation regimes. *Sci. Rep.*, **4**, 4364, https://doi.org/10.1038/srep04364.

Rutz, J. R., and Coauthors, 2014: Climatological characteristics of atmospheric rivers and their inland penetration over the western United States. *Mon. Wea. Rev.*, **142**, 905–921, https://doi.org/10.1175/MWR-D-13-00168.1.

St. George, S., and T. R. Ault, 2011: Is energetic decadal variability a stable feature of the central Pacific Coast's winter climate? *J. Geophys. Res.*, **116**, D12102, https://doi.org/10.1029/2010JD015325.

——, and ——, 2014: The imprint of climate within Northern Hemisphere trees. *Quart. Sci. Rev.*, **89**, 1–4, https://doi.org/10.1016/j.quascirev.2014.01.007.

Stahle, D. W., M. D. Therrell, M. K. Cleaveland, D. R. Cayan, M. D. Ettinger, and N. Knowles, 2001: Ancient blue oaks reveal human impact on San Francisco Bay salinity. *Eos, Trans. Amer. Geophys. Union*, **82**, 141–145, https://doi.org/10.1029/EO082i012p00141.

——, and Coauthors, 2013: The blue oak woodlands of California: Longevity and hydroclimatic history. *Earth Interact.*, **17**, https://doi.org/10.1175/2013EI000518.1.

Steinschneider, S., M. Ho, E. R. Cook, and U. Lall, 2016: Can PDSI inform extreme precipitation?: An exploration with a 500 year long paleoclimate reconstruction over the U.S. *Water Resour. Res.*, **52**, 3866–3880, https://doi.org/10.1002/2016WR018712.

——, ——, A. P. Williams, E. R. Cook, and U. Lall, 2018: A 500-year tree-ring based reconstruction of extreme cold-season precipitation and number of atmospheric river landfalls across the Southwestern U.S. *Geophys. Res. Lett.*, **45**, 5672–5680, https://doi.org/10.1029/2018GL078089.

Stuivenolt-Allen, J., S.-S. Wang, Z. Johnson, and Y. Chikamoto, 2021: Atmospheric rivers impacting northern California exhibit a quasi-decadal frequency. *J. Geophys. Res. Atmos.*, **126**, e2020JD034196, https://doi.org/10.1029/2020JD034196.

Swain, D. L., B. Langenbrunner, J. D. Neelin, and A. Hall, 2018: Increasing precipitation volatility in twenty-first-century California. *Nat. Climate Change*, **8**, 427–433, https://doi.org/10.1038/s41558-018-0140-y.

Torrence, C., and G. P. Compo, 1998: A practical guide to wavelet analysis. *Bull. Amer. Meteor. Soc.*, **79**, 61–78, https://doi.org/10.1175/1520-0477(1998)079<0061:APGTWA>2.0.CO;2.

Wahl, E. R., A. Hoell, E. Zorita, E. Gille, and H. F. Diaz, 2020: A 450-year perspective on California precipitation "flips." *J. Climate*, **33**, 10 221–10 237, https://doi.org/10.1175/JCLI-D-19-0828.1.

Warner, M. D., C. F. Mass, and E. P. Salathe Jr., 2015: Changes in winter atmospheric rivers along the North American west coast in CMIP5 climate models. *J. Hydrometeor.*, **16**, 118–128, https://doi.org/10.1175/JHM-D-14-0080.1.

Williams, A. P., K. J. Anchukaitis, C. A. Woodhouse, D. M. Meko, B. I. Cook, K. Bolles, and E. R. Cook, 2021: Tree rings and observations suggest no stable cycles in Sierra Nevada cool-season precipitation. *Water Resour. Res.*, **57**, e2020WR028599, https://doi.org/10.1029/2020WR028599.